


## Article

# The Smart Detection of Ship Severe Roll Motions and Decision-Making for Evasive Actions

Maria Acanfora \* and Flavio Balsamo 

Department of Industrial Engineering, University of Naples “Federico II”, 80125 Napoli, Italy;  
flavio.balsamo@unina.it

\* Correspondence: maria.acanfora@unina.it

Received: 30 April 2020; Accepted: 4 June 2020; Published: 6 June 2020



**Abstract:** This paper presents a numerical model for the smart detection of synchronous and parametric roll resonance of a ship. The model implements manoeuvring equations superimposed onto ship dynamics in waves. It also features suited autopilot and rudder actuator models, aiming at a fair depiction of the control delay. The developed method is able to identify and distinguish between synchronous and parametric roll resonance, based on the estimation of encounter wave period from ship motions. Therefore, it could be useful as a smart tool for manned vessels and, also, in the perspective of unmanned and autonomous vessels (in the paper it is assumed a hypothetical remote crew). Once the resonance threat is identified, different evasive actions are simulated and compared, based on course and speed change. Calculations are carried out on a ro-ro pax vessel vulnerable to parametric roll. We conclude that, in roll resonance situations, and in the absence of roll stabilisation systems on-board, course change could be the most effective countermeasure.

**Keywords:** ship dynamics; ship manoeuvring; numerical simulations; parametric and synchronous roll; smart vessels

## 1. Introduction

Recent interest in smart ships brings out new possibilities in vessel operations but, at the same time, involves new challenges [1,2]. Regarding the smart tool development for supporting crew decisions on manned ships, the smart vessel concept extends to unmanned and autonomous ships with several levels of automation. The unmanned ship is expected to be operated by remote actions since there would be no crew on-board. Therefore, the vessel has to be equipped with an extensive set of sensors concerning videos, acceleration and motion tracking, accounting for redundant tools [3,4]. The decision-making processes performed by the crew, conventionally based on physical perceptions, have to be moved to a digital perception of the reality. The autonomous ship is expected to operate without any human action, independently from the presence of crew on-board. The vessel is provided with smart tools capable of elaborating sensor signals and making decisions on ship routing and operation, autonomously. This is particularly relevant for decision-making processes, conventionally performed by humans, and the resulting choices.

One of the main concerns about smart vessels regards the assessment of ship safety [5–7], with the development and establishment of dedicated rules. Such regulations on autonomous/remote ships are currently under development by the classification societies [8]. The ship usually faces several troublesome situations during navigation. This paper focuses on excessive motions arising from parametric and synchronous roll, that are responsible for large accelerations with severe consequences for ship safety. Parametric roll resonance depends on the variation of the immersed hull in waves and can happen mainly in head/following seas, but even in oblique waves. The most severe condition for triggering parametric resonance is characterised by an encounter wave period that is half of the natural

roll period. Weaker parametric resonance also can be observed for an encounter wave period equal to a natural roll period, although this might be confused with synchronous roll resonance, especially in oblique seas. Indeed, synchronous roll resonance, depending on the agreement of encounter wave period and natural roll period, can happen for oblique and beam waves, while for head and following seas no roll motion is expected. Herein, weaker parametric resonance scenarios (characterised by a natural roll period equal to the wave period) are not under investigation, nevertheless, the developed method is expected to identify them as synchronous roll threats. Specifically, ships prone to parametric roll could develop large roll motions and, thus, lead to dangerous scenarios such as cargo shifting [9,10] or even capsizing. Nevertheless, synchronous roll, which indeed can happen more frequently and for all ship types, could lead to unpleasant consequences [11,12].

Considering the perspective of a smart ship, according to the guidelines developed by DNV-GL [8], a breakdown of ship functions involves the following features: condition detection, condition analysis, action planning and action control (i.e., execution). Route planning is an important aspect to take care of since it aims at critical scenario forecasting before setting out to sea. Regarding the avoidance of excessive roll motions and accelerations, route planning mainly employs polar diagrams or similar methods [13–17]. However, it has been recognised that real-time applications of such tools for condition detection and analysis would be difficult [18], especially when a ship navigates in unexpected or accidental operational conditions not covered by the diagrams. Several methods were developed and presented by the authors of [19–22] mainly for the detection of parametric roll resonance, aiming at providing on-board decision support systems during navigation. However, they disregard the synchronous roll. Dealing with roll resonance phenomena, the measurement and identification of the wave period and heading during navigation are crucial. One of the novel aspects of this paper is the development of a reliable autonomous system, able to replace the crew perception of the sea state, aiming at the detection and analysis of the resonance threats. The research focuses on three different approaches for determining encounter wave periods in irregular waves, based on the measurements of heave and pitch motions. This follows the idea of exploiting ship motions as estimators of sea state characteristics [23,24]. These three approaches refer respectively to: FFT (Fast Fourier Transform) analysis, time-domain assessment, and Hilbert transform. Except for the Hilbert-based approach, the first two were already introduced in a previous research paper [25], where they were applied separately. Herein, all three proposed approaches are simultaneously applied and compared, aiming at the evaluation of a more reliable prediction. Therefore, the current paper concerns the enhancement of an autonomous routine for condition detection and analysis; moreover, it also aims at providing novel insights regarding action planning and control execution that, for the purpose of the paper, are assumed up to the crew. Indeed, in the reference paper [25], the analysis was limited to the identification of the excessive roll motion threats once the whole time history was achieved from the numerical simulations, with no possibility of controlling the speed and heading of the vessel during the run. The first part of the current research deals with the implementation of the method for condition detection and analysis within the time domain simulations for real-time threat identification. The investigation of action planning and control execution features the development of a numerical model that includes the main ship control systems for executing the evasive action by modifying the speed or course. The latter requires the implementation of the rudder actuator and autopilot models [26]. This implementation aims at enhancing the estimation of ship behaviour once the control is executed. The outcomes of selected case studies, involving the detection of parametric and synchronous roll resonance, followed by the executions of different evasive actions, provide novel knowledge on the best countermeasure to different critical scenarios.

The ship under study is a ro-ro pax ferry named Seatech-D. Despite the smart tool developed herein being intended for both manned and unmanned ships, it might be questioned that a passenger ferry is not a realistic candidate for becoming an unmanned or autonomous vessel for near-future industrial applications. Indeed, in this research, the hull is mainly used for testing the developed method: regarding Seatech-D, experimental campaign data regarding a self-propelled turning circle in

irregular waves and straight runs in oblique irregular waves are available [27,28]. Therefore, for the scope of the current applications, it is considered appropriate.

The paper is structured as follows. First, a brief description of the numerical model for ship dynamics is given, with particular relevance to the rudder and steering actions. Then, the parametric and synchronous roll detection routine is applied to the numerical simulations. Once a threat is identified, the control of the vessel is performed and the obtained results on evasive actions are further discussed. Finally, conclusions are drawn.

## 2. Numerical Model for Ship Control in Irregular Waves

The numerical model is based on a combination of sea-keeping and manoeuvring motions in irregular seas, as presented by the authors of [29,30], accounting for all the pertinent non-linearities. The previous researches employed the computer program LAIDYN coded in Fortran [29], well known in the technical literature and validated through several benchmark studies [31–33]. Differently, the current numerical model is implemented in a Matlab/Simulink environment and it features novel approaches regarding autopilot and steering actions, thus aiming at a more realistic application of ship control attitude in adverse sea states.

A suitable superposition of sea-keeping and manoeuvring motions guarantees a fair agreement of the numerical outcomes with the available experimental data. This is carried out by assuming that the added mass coefficients for an infinite frequency are valid for both sea-keeping and manoeuvring models; while the damping coefficients, corresponding to the sway–yaw motions, refer only to the manoeuvring derivatives (i.e., radiated wave effects are excluded). The damping actions, in the remaining degrees of freedom, are implemented by the convolution integral technique [34]. Rudder forces develop in agreement with the instantaneous angle of attack and speed at the blade location, as explained by the authors of [29,30]. Differently from the reference papers, the effects of propeller action on the rudder flow are disregarded herein. This would induce an error on the velocity at the rudder blade, while in the current simulations no appreciable differences were found by comparing the numerical and the experimental turning circle results. Concerning the scope of the research, the small approximation regarding the propeller action on the rudder flow is considered tolerable.

The propeller thrust is achieved by a fixed revolution approach, which involves a modification of the ship speed due to the wave actions. The obtained wave resistance in the numerical simulation (i.e., all wave actions in the x-axis, body reference frame), does not account for second-order effects. The current numerical model gives the possibility to modify ship heading (through rudder deflection) and propeller revolution during the simulation. Particularly, the rudder angle changes accounting for a realistic delay in both the autopilot and the steering control laws.

The main objective of ship manoeuvring is to control the heading angle of the ship. This is conventionally carried out, in the majority of vessels, by rudder actions that ensure course keeping and course change. The control system must alter the control surfaces to a desired heading angle; the rudder deflection angle can be set manually (as usually done by the helmsman) or autonomously employing an autopilot. The current model implements a PID (proportional, integral, derivative) autopilot, capable of controlling rudder deflection to achieve the desired heading angle. The proportional, integral and derivative constants are set by the “trial and error” approach, to ensure a suitable control action in waves; the integral action is almost negligible compared to the others.

It is important to underline that the desired rudder angle, as required by the autopilot, cannot be achieved instantaneously due to the damping (provided by the surrounding fluid) and the inertia (due to the rudder shape and weight distribution). Thus, the torque for turning the rudder, provided by a hydraulic actuator, has to compensate for several effects and the rudder turn dynamics are modelled by a second-order linear system. This aims at a more realistic control approach [26].

### 3. Case Study

The ship under investigation is a monohull ro-ro pax ferry, named Seatech-D, whose main particulars are given in Table 1. This hull was developed and investigated at the Aalto University in terms of resistance, stability, and sea-keeping tests. Additional details can be found in Stigler and Matusiak [28,29]. Particularly, for section plans and ship drawings refer to Stigler [28].

**Table 1.** Principal particulars of Seatech-D.

Dimension/Hull	Seatech-D
Length between perpendiculars, L (m)	158.00
Breadth, B (m)	25.00
Depth, D (m)	15.00
Draft forward, $T_F$ (m)	6.10
Draft aft, $T_A$ (m)	6.10
Displacement, $\Delta$ (tons)	13,766
Center of gravity above keel, KG (m)	11.834
Long. coordinate of the center of gravity measured from aft perpendicular, LCG (m)	74.77
Transv. radius of gyration in air, $k_{XX}$ (m)	10.06
Long. radius of gyration in air, $k_{YY}$ (m)	39.36

Concerning this hull, experimental data regarding straight runs in oblique seas and turning circles in irregular waves are available [27,28]. The hull model is not equipped with bilge keels.

The comparisons with the straight runs in oblique waves have been already presented [11], showing a fine match of the results (assessed by superposition of the numerical and experimental data, checking the agreement of the overlapping curves). Figure 1 shows a turning circle simulation, carried out by the numerical model under development herein. Irregular sea refers to JONSWAP spectrum with a zero-crossing period  $T_Z = 5.5$  s, and significant wave height  $H_S = 4.8$  m, and it is discretised by  $N = 30$  wave components; ship speed is set  $V_S = 8.40$  m/s and rudder deflection is  $\delta = 20^\circ$  (in ship scale). Turning path results are in model scale 1:39, the remaining outcomes refer to ship scale. There is an overall fair agreement between the turning diameter and the roll motion behaviour, as observed from the reference experimental and numerical data [27,28].

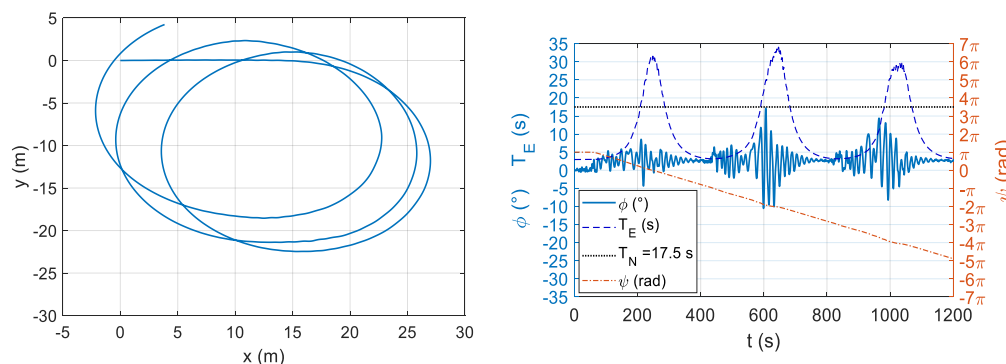


**Figure 1.** Turning circle in irregular waves (JONSWAP  $T_Z = 5.5$  s,  $H_S = 4.8$  m,  $N = 30$  wave components,  $V_S = 8.40$  m/s,  $\delta = 20^\circ$  in ship scale). Turning path on the left-hand side (model scale); Roll and sway angles on the right-hand side (ship scale).

All details about the turning circle conditions are given (in ship scale) in the Figure 1 caption. The ship performs three turns in less than 1200 s and, consequently, she experiences three times an amplification of the roll motions due to the resonance between the natural roll period ( $T_N = 17.5$  s) and encounter period  $T_E$ . The latter accounts for the variation of wave heading and ship speed during the turn. This test ensures the reliability of the implemented models for rudder actions (for a constant deflection) and ship manoeuvring, superimposed onto the vessel dynamics in irregular waves.

The rudder actuator model implements inertia, damping, restoring and PID coefficients that are needed for the rudder turn execution, derived from design considerations. These coefficients are assumed to ensure that the time to deflect the rudder in still water from  $\delta = -30^\circ$  to  $\delta = 35^\circ$  remains below 28 s [35], in the absence of detailed data. A numerical application of this deflection test for Seatech-D is shown in Figure 2: rudder deflection starts from  $\delta = -30^\circ$  at 101 s and reaches approximately  $\delta = 35^\circ$  at 127 s. The rate of turn  $\dot{\delta}$  does not exceed 7.5 deg/s.

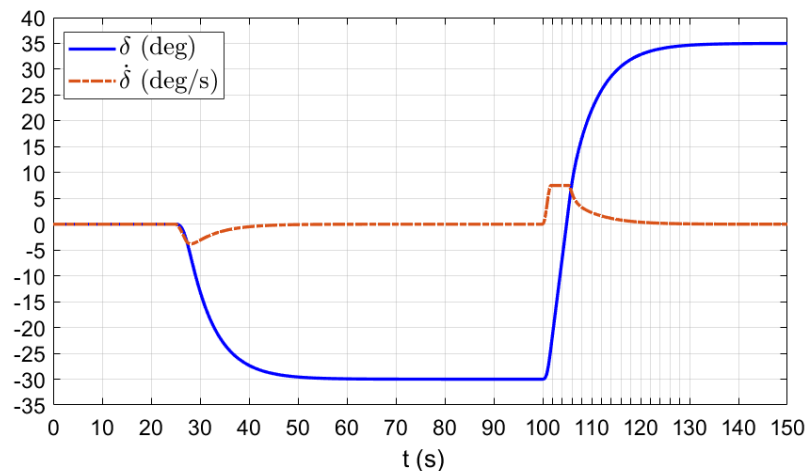


**Figure 2.** Example of a rudder deflection test from  $-30^\circ$  to  $35^\circ$  at operational speed in still water.

Despite the simplifying assumptions adopted herein, the outcomes of the turning circle and rudder deflection tests provide a satisfactory behaviour of the numerical model in representing ship dynamics and the steering action in a realistic manner.

### 3.1. Autonomous Detection of the Excessive Roll Motions

The autonomous detection system for excessive roll threats in severe seas features a constant monitoring of the sea state, i.e., it estimates the wave encounter period through measurements and analysis of heave and pitch motions. The system measures roll motions alongside, focusing on average roll amplitude, and all data are processed every 90 s. Once the estimated wave encounter period falls within 40–60% (or 80–120%) of the known natural period ( $T_N$ ) of the ship, and mean roll amplitude exceeds a certain threshold, the autonomous detection system forwards an alert signal of parametric (or synchronous) roll. This alert could be sent to an on-board crew or a remote one, depending on a manned or unmanned ship (in the remaining of the paper it is assumed a hypothetical remote crew). This resembles the first part of the approach developed by Acanfora [25], i.e., autonomous detection and alert identification.

Following the alert signal, the crew examines the ship behaviour and operational condition and, consequently, it takes an evasive action by changing the speed (controlling the propeller revolution) or by changing the heading (setting the autopilot and, thus, affecting rudder deflection). The simulation of the countermeasure actions and the corresponding effectiveness analysis represent the novel aspect of this research. Besides, in the current applications, it is assumed that the crew always takes an evasive action once a roll resonance threat is detected, although it could decide not to intervene.

### 3.2. Techniques for Monitoring Encounter Wave Period and Roll Amplitude

The need for a reliable assessment of the encounter wave period is directly correlated to a correct interpretation of the reason behind the development of large roll motions. When the encounter period of the waves and the natural roll period of the ship fall close to the ratio 1:2 (that is  $T_E = T_N/2$ ), with large roll amplitudes even in relatively moderate wave heights, then a parametric resonance could reasonably be identified. Pitch and heave motions are adopted as indicators of sea state by processing

the time history samples every 90 s with a frequency of 5 Hz. Indeed, these are two signals that exhibit a well-established linear behaviour, related to the encounter wave period. The peak periods of each sample of pitch and heave ( $\bar{T}_\theta$  and  $\bar{T}_\zeta$  respectively) are assumed as the current encounter wave period  $\bar{T}_w$ . The adoption of three techniques for each signal, listed and briefly explained below, can help in identifying the most reliable approach and can improve redundancy. FFT analysis ( $\bar{T}_\theta$  and  $\bar{T}_\zeta$  are the peak values of the pitch and heave spectra, obtained by the 90 s samples of pitch and heave, respectively). Mean period of the peaks from the time history ( $M$  is the number of the peaks, referring to heave-subscript  $\zeta$  and pitch-subscript  $\theta$  respectively, within the 90 s samples):

$$\begin{cases} \bar{T}_\zeta = \frac{1}{M_\zeta} \sum_{i=1}^{M_\zeta} T_{\zeta,i} \\ \bar{T}_\theta = \frac{1}{M_\theta} \sum_{i=1}^{M_\theta} T_{\theta,i} \end{cases}$$

Hilbert transform analysis of pitch  $\theta(t)$  and heave  $\zeta(t)$  samples [36]:

$$\begin{aligned} z_\theta &= \theta(t) + iH[\theta(t)] = \theta(t) + i\frac{1}{\pi}P.V. \int_{-\infty}^{+\infty} \frac{\theta(\tau)}{t-\tau} d\tau = A_\theta(t)e^{ik_\theta(t)} \\ \bar{T}_\theta &= 1/T \int_T \frac{2\pi}{dk_\theta(t)/dt} d\tau \\ z_\zeta &= \zeta(t) + iH[\zeta(t)] = \zeta(t) + i\frac{1}{\pi}P.V. \int_{-\infty}^{+\infty} \frac{\zeta(\tau)}{t-\tau} d\tau = A_\zeta(t)e^{ik_\zeta(t)} \\ \bar{T}_\zeta &= 1/T \int_T \frac{2\pi}{dk_\zeta(t)/dt} d\tau \end{aligned}$$

where  $A$  is the signal instantaneous amplitude and  $k$  is the signal instantaneous phase, referring to heave-subscript  $\zeta$  and pitch-subscript  $\theta$  respectively, within the 90 s samples.

Along these lines, three values of the period for each motion sample are available. Redundant values of  $\bar{T}_w$ , estimated utilising  $\bar{T}_\theta$  and  $\bar{T}_\zeta$ , can be achieved. A single value of the period is obtained as a mean value among the three; however, in the case of a large disagreement among them, they are considered separately.

The parametric roll (PAR) alert is set as follows:

$$PAR_{index} = \begin{cases} 1 & \text{if } \phi_A \geq \phi_{alert} \text{ and } 0.4 < \bar{T}_w/T_N < 0.6 \\ 0 & \text{if } \phi_A < \phi_{alert} \end{cases}$$

where  $\phi_A$  is the average value of roll amplitude, estimated from the measurement of roll motion in the same time range of heave and pitch. Thus, the Hilbert transform approach is employed:

$$z_\phi = \phi(t) + iH[\phi(t)] = \phi(t) + i\frac{1}{\pi}P.V. \int_{-\infty}^{+\infty} \frac{\phi(\tau)}{t-\tau} d\tau = A_\phi(t)e^{ik_\phi(t)} \quad \phi_A^2 = 1/T \int_T A_\phi^2(t) d\tau$$

When there is a scenario involving synchronous (S) roll resonance, the corresponding alert index is set as:

$$S_{index} = \begin{cases} 1 & \text{if } \phi_A \geq \phi_{alert} \text{ and } 0.8 < \bar{T}_w/T_N < 1.2 \\ 0 & \text{if } \phi_A < \phi_{alert} \end{cases}$$

Regarding an alert scenario, a threshold value between 10–15° should be expected [25]. Since this alert refers to possible developments of roll resonance in an early stage, a moderate roll amplitude is



considered adequate for setting the alert. During the current simulation, it is set to  $\phi_{alert} = 12.5^\circ$ , as a mean value between  $10\text{--}15^\circ$ .

## 4. Results and Discussions

### 4.1. Parametric Roll Scenario

The autonomous detection technique operates on two redundant wave period values (one on the heave, one on the pitch, as mean values among the three techniques introduced above); therefore, two alert indexes are provided. When at least one of these two values becomes equal to one, then the system forwards the alert signal immediately to the remote crew. Once the alert is sent, the reaction time would depend on the preparedness of the remote crew, while the control action would depend on its expertise and experience.

The following applications show an example of the autonomous detection of large parametric roll motions together with some possible remote crew actions. The case study involves an irregular sea state modeled by a JONSWAP spectrum with  $H_S = 4.5$  m and  $T_Z = 9.5$  s (peak period  $T_P = 12.2$  s). It is implemented by exploiting the technique proposed by Acanfora [11], adopting  $N = 30$  wave components. This irregular sea scenario, together with a ship sailing in the head sea direction with a speed of  $V_S = 8.4$  m/s (that is around 16 knots), can lead to the development of parametric roll. The initial ship heading in the simulation, is set at  $\psi = 175^\circ$  to introduce a small perturbation (for a faster development of parametric resonance within the numerical model). The autonomous detection technique applies to the sample critical scenario, regarding which the remote crew might intervene with three different actions to modify the operational condition: change of heading of  $15^\circ$ , change of heading of  $30^\circ$  or speed reduction of 5 knots. Concerning a fair comparison between the outcomes, each numerical run is based on the same wave realisation. Figure 3 shows the effects on ship dynamics when changing the vessel course of  $15^\circ$ . Figure 3A (left-hand side) regards ship dynamics and control actions, while Figure 3B (right-hand side) focuses on the alert detection and on the effects of the control application. It is possible to observe that large roll motions, in head sea, start developing after 12 min of navigation (i.e., around 720 s). The  $PAR_{index}$  becomes equal to 1, i.e., the alert signal is sent to the remote crew, with 90 s of delay. This corresponds to the sample time that the system takes to assess the current alert state of the ship.

Regarding these applications, in the absence of precise and dedicated data, it is assumed that the remote operator reacts within 30 s after the alert signal and quickly sets the autopilot to change the course by  $15^\circ$ . The ship change of heading to  $\psi = 160^\circ$  does not produce any appreciable change to roll motions i.e., the hull is still within the parametric resonance condition. An additional change of course by  $15^\circ$ , leading to  $\psi = 145^\circ$ , is effective in bringing the hull out of resonance, with moderate roll motions. Under such circumstances, it takes time to judge that the first change of heading was ineffective, thus, parametric roll lasts quite a long time before moving out from the resonance range. The best approach, in terms of incisive countermeasures to parametric roll, is the immediate change of course by  $30^\circ$ , soon after the alert is identified (see Figure 4). Once the command is fed to the autopilot, the  $PAR_{index}$  returns to zero after 4 min, which means that the parametric roll extinguishes after 2.5 min (i.e., 90 s in advance of the  $PAR_{index}$ ). However, this choice would result in a quite significant re-scheduling of the ship route, although it guarantees a quick and effective action.

Another feasible approach, to avoid route modification, is the action involving a speed reduction, thus tolerating a slowdown due to the adverse weather conditions. Seen in Figure 5, a speed reduction of 5 knots is adopted as a countermeasure against parametric roll. However, the results in Figure 5A (left-hand side) and Figure 5B (right-hand side) show that this approach is not fully effective. The roll motion mitigates, but it does not extinguish completely. This is supported by the evidence that the  $PAR_{index}$  does not remain equal to zero after the speed reduction (especially the  $PAR_{index}$  related to pitch motion). Therefore, among the proposed actions, the speed reduction appears the least reliable and the least safe. A further reduction in speed would not guarantee a feasible alternative, not only

from a routing point of view, it would be detrimental for vessel directional stability and course keeping, also leading to less dampened ship motions.

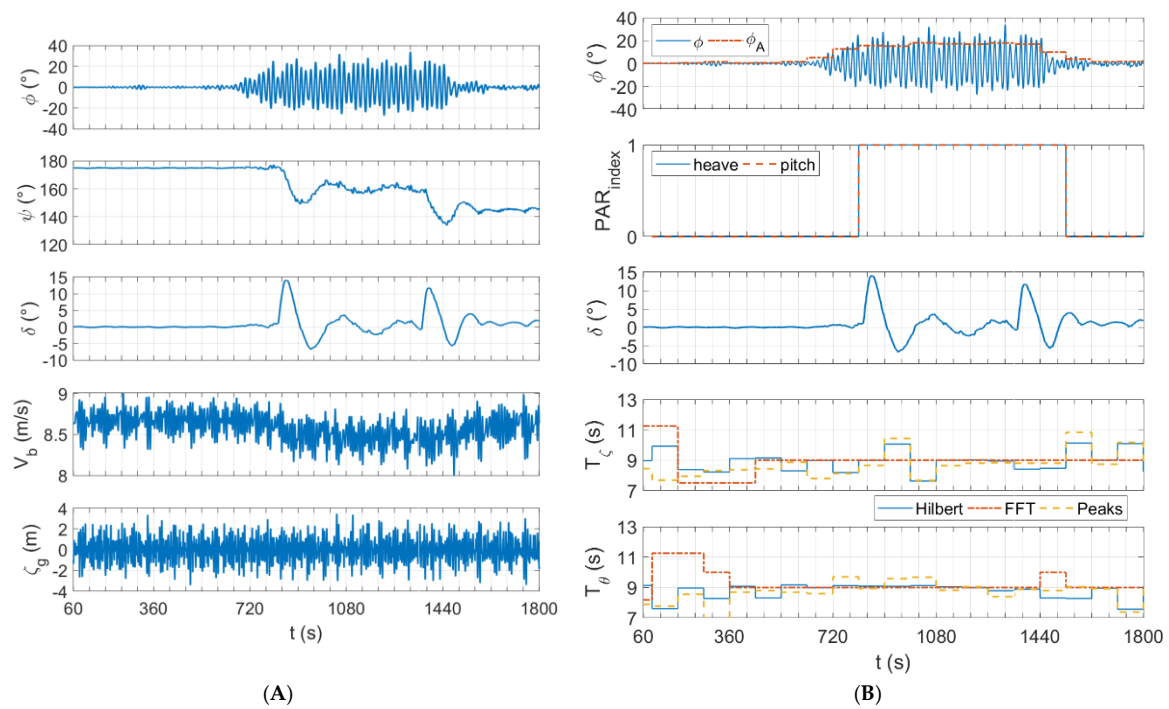


**Figure 3.** Parametric roll and course change of 15° plus 15° in irregular waves (JONSWAP  $T_Z = 9.5$  s,  $T_P = 12.2$  s,  $H_S = 4.5$  m,  $N = 30$ ,  $V_S = 8.40$  m/s,  $\psi = 175^\circ$ ). (A) Ship dynamics outcomes; (B) Alert and control outcomes.

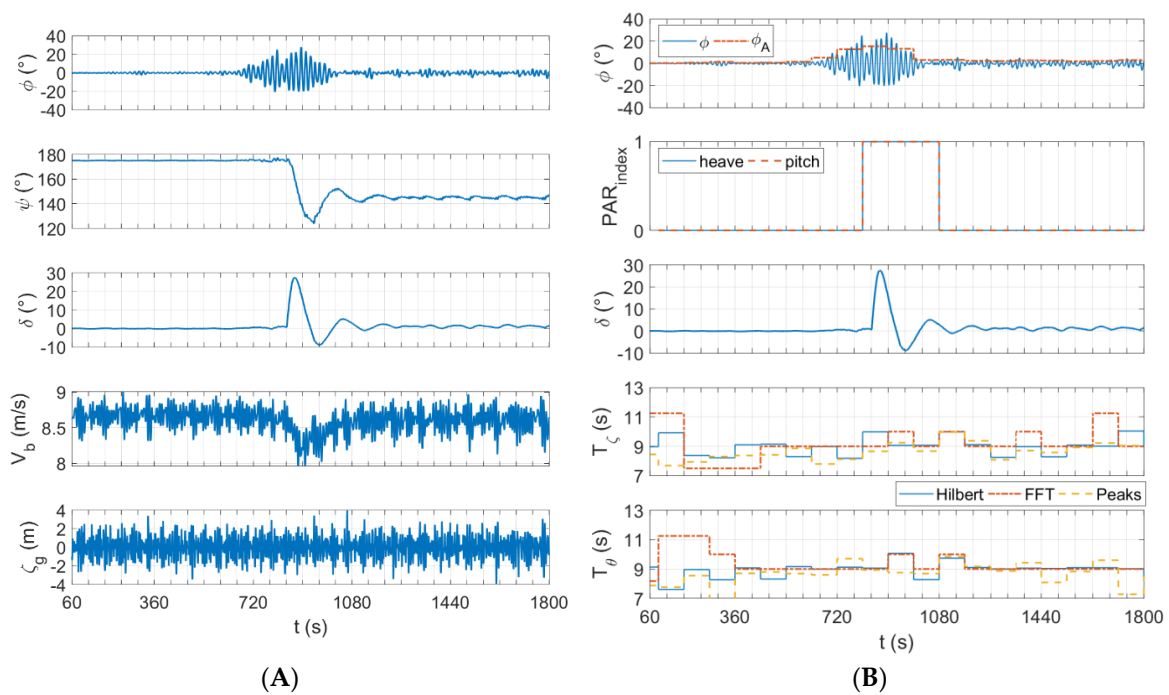


**Figure 4.** Parametric roll and course change of 30° in irregular waves (JONSWAP  $T_Z = 9.5$  s,  $T_P = 12.2$  s,  $H_S = 4.5$  m,  $N = 30$ ,  $V_S = 8.40$  m/s,  $\psi = 175^\circ$ ). (A) Ship dynamics outcomes; (B) Alert and control outcomes.



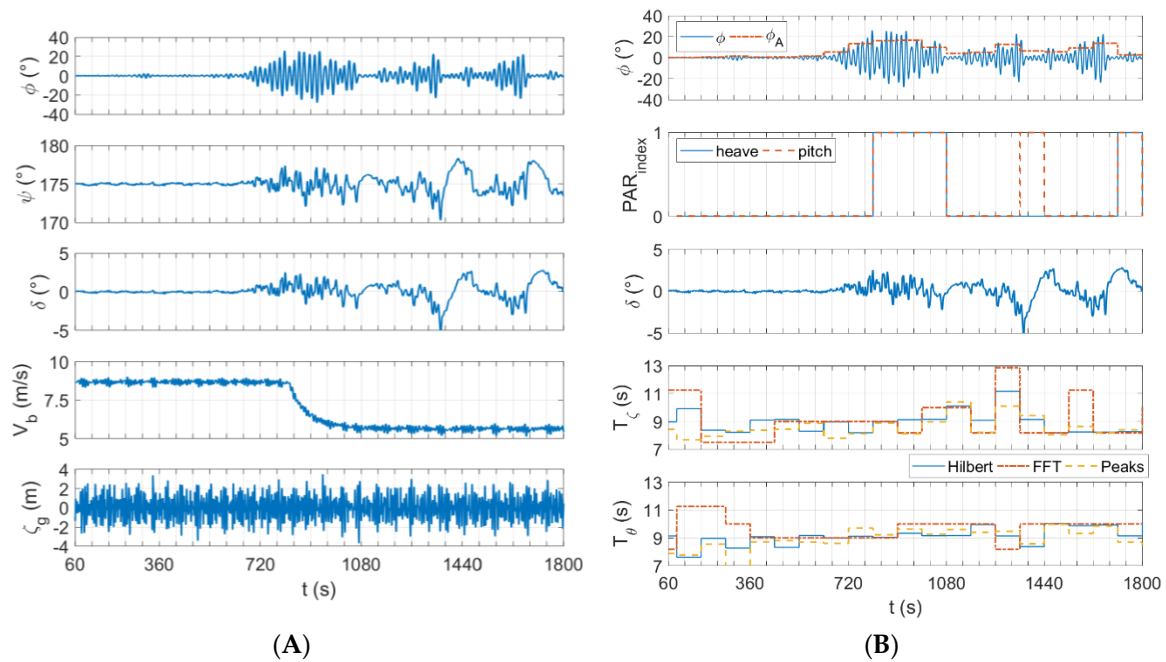


**Figure 5.** Parametric roll and speed reduction in irregular waves (JONSWAP  $T_Z = 9.5$  s,  $T_P = 12.2$  s,  $H_S = 4.5$  m,  $N = 30$ ,  $V_S = 8.40$  m/s,  $\psi = 175^\circ$ ). (A) Ship dynamics outcomes; (B) Alert and control outcomes.

#### 4.2. Synchronous Roll Scenario

Large roll motions can generally arise in the event of synchronous resonance. This phenomenon is critical for all ship types and it is a more frequent issue during ship navigation than parametric roll resonance. Therefore, the autonomous detection system has to provide alerts also in the case of synchronous roll threats.

Synchronous resonance is found for the operational condition in irregular sea characterised by  $T_Z = 5.5$  s (peak period  $T_P = 7.1$  s),  $H_S = 6$  m, with ship speed  $V_S = 8.40$  m/s and heading  $\psi = 45^\circ$ . While for parametric roll case all three techniques provided comparable periods, thus improving the redundancy of the system, actually this is not confirmed by the outcomes of synchronous resonance case. Figure 6 yields an overview of the accuracy of the wave period estimation related to the alert index  $S_{index}$ . It appears that  $\bar{T}_w$ , obtained as the mean value among FFT, Hilbert and Peak calculated periods, leads to underestimated alert conditions. Indeed, if we evaluate the  $S_{index}$  separately for every single period, the FFT-based value is the most effective in alert detection, although it shows a larger variation in time. Conversely, the Peak-based value does not provide any alert signal in the whole time range. However, all approaches fail around 200–300 s, when  $\phi_A$  exceeds  $12.5^\circ$ , and none of them identifies the alert. This issue also could be linked to the heading corresponding to the case study. The parametric resonance case was investigated in the head sea range, where heave and pitch motions are predominant, while the synchronous resonance case was investigated in the stern-quartering sea, where all motions develop. Moreover, the latter case also included larger autopilot actions for course keeping in oblique waves, characterized by low-frequency manoeuvring motions. All this might affect the fine development of heave and pitch motions in accordance with the wave period, when the ship operates in the stern-quartering sea. Nevertheless, these considerations bring out some limits in the proposed techniques that should be further analysed for assessing the most robust approach.

Alternatively, the alert could be assessed by focusing on roll amplitude only, leaving the autonomous detection of  $S_{index}$  versus  $PAR_{index}$  as discretionary indicators. Thus, the remote crew should judge between synchronous or parametric resonance by looking at the different weights of  $\bar{T}_w$ . Nevertheless, based on the application outcomes for the Seatech-D hull, the identification of the type of resonance has a great relevance in the type of countermeasure to adopt.

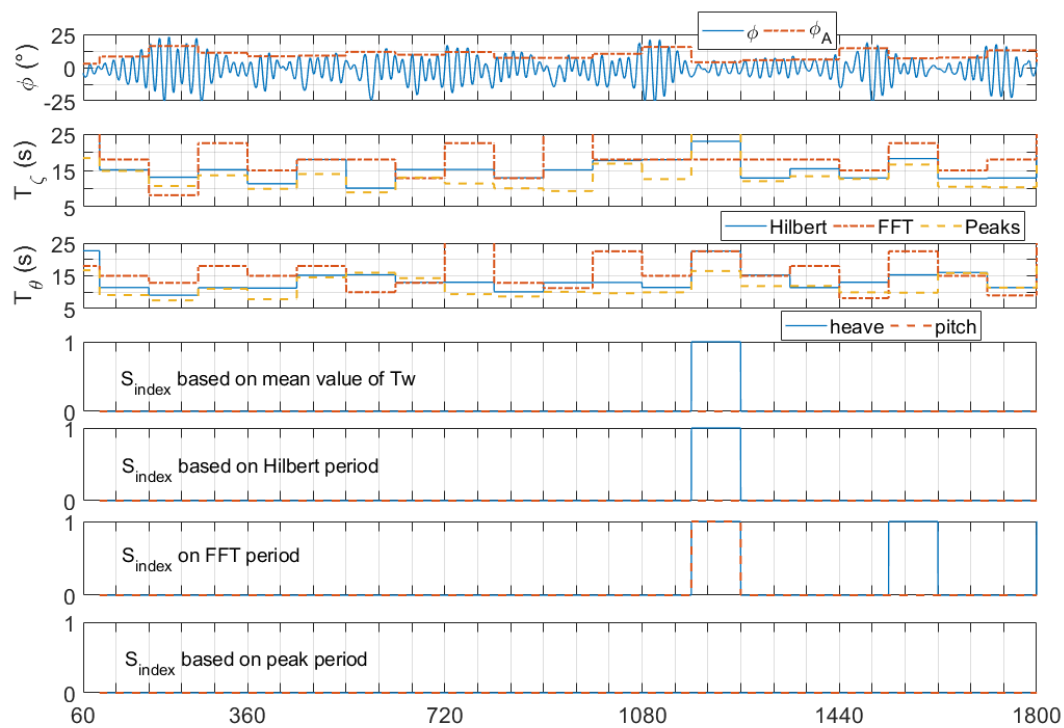


**Figure 6.** Synchronous roll and comparison of alert based on wave period estimation; irregular waves (JONSWAP  $T_Z = 5.5$  s,  $T_P = 7.1$  s,  $H_S = 6$  m,  $N = 30$ ,  $V_S = 8.40$  m/s,  $\psi = 45^\circ$ ).

Particularly, once the alert is provided (around 1200 s) it appears that synchronous roll resonance extinguishes more easily than parametric resonance. Indeed, small changes in the heading (see Figure 7) and a modest reduction in ship speed (see Figure 8) guarantee the resolution to large roll motions. Figure 7 shows the dynamics of the ship to a course change of  $15^\circ$  given at 1230 s: roll amplitudes reduce significantly.

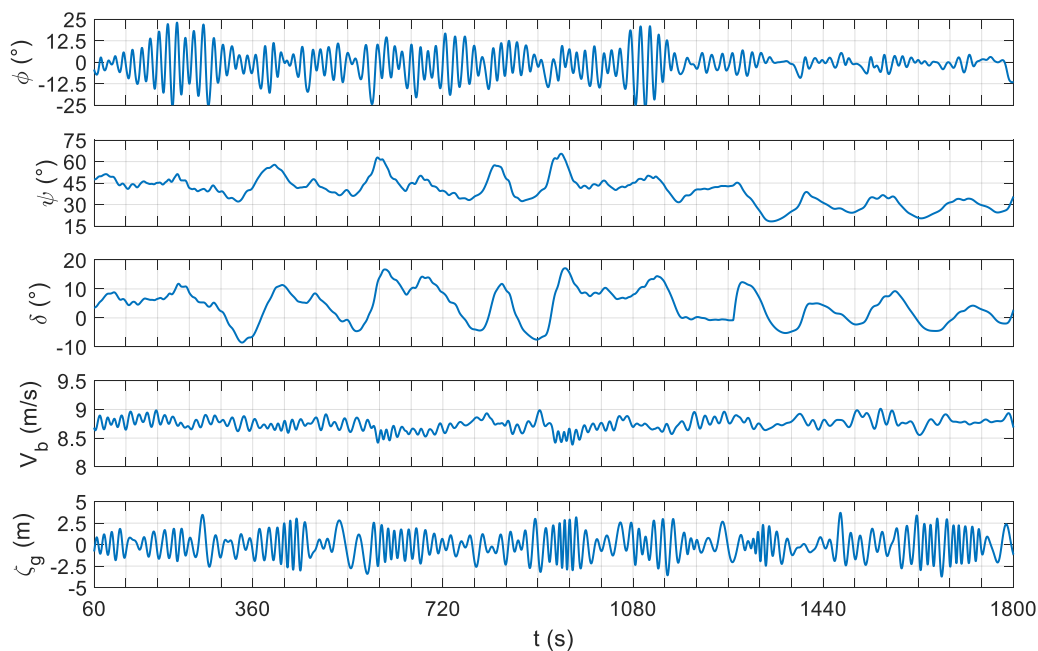


**Figure 7.** Synchronous roll avoidance by a course change of  $15^\circ$ ; irregular waves (JONSWAP  $T_Z = 5.5$  s,  $T_P = 7.1$  s,  $H_S = 6$  m,  $N = 30$ ,  $V_S = 8.40$  m/s,  $\psi = 45^\circ$ ).

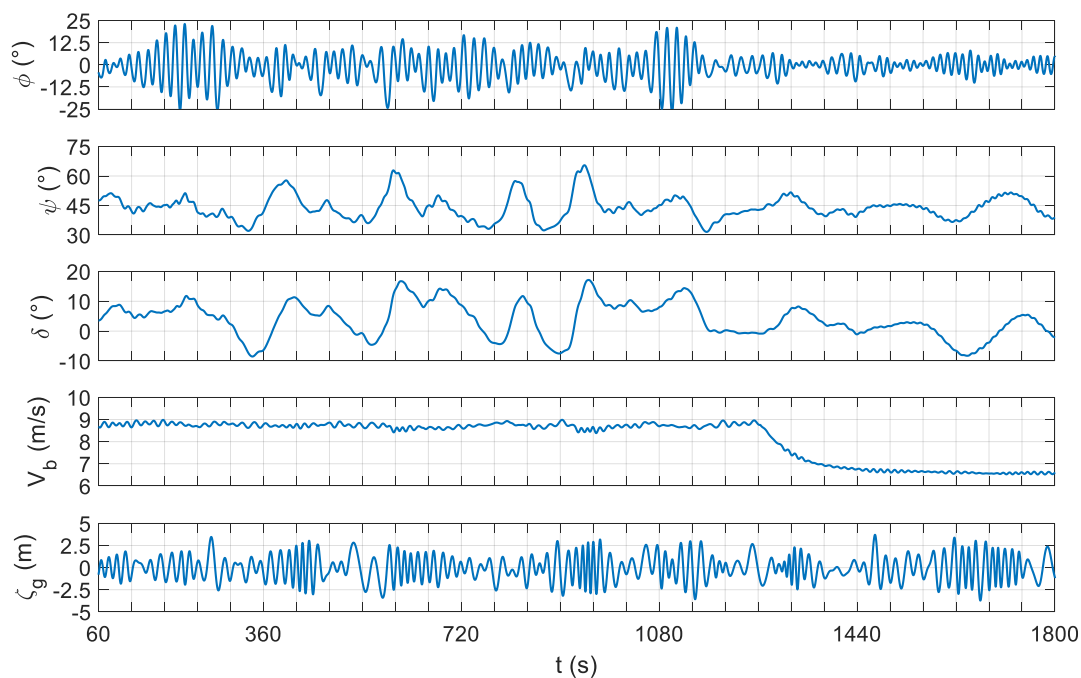


**Figure 8.** Synchronous roll avoidance by a speed reduction of 3.5 knots; irregular waves (JONSWAP  $T_Z = 5.5$  s,  $T_P = 7.1$  s,  $H_S = 6$  m,  $N = 30$ ,  $V_S = 8.40$  m/s,  $\psi = 45^\circ$ ).

It is possible to observe that the oblique sea navigation requires a demanding rudder control for the course keeping in waves. This also is appreciable in Figure 8, where no course change is expected, but the rudder still has to operate to keep the initial heading. Moreover, Figure 8 points out that a speed reduction of around 3.5 knots is as effective as a course change in mitigating roll motions. Small deviations to initial operational conditions appear sufficient to react to synchronous resonance.

## 5. Conclusions

In this paper novel techniques for the smart assessment of large roll motions were implemented by a numerical simulation model trained to idealize the influence of evasive actions on ship dynamics. Parametric and synchronous roll resonance threats were investigated as applied to a ro-ro pax ship.

The estimation of the wave encounter period exploited the use of the ship as a floating buoy: short records of pitch and heave motions were processed in three different ways for monitoring their periods that, in our analysis, correspond to wave periods. The differences among the three adopted techniques appeared more pronounced for the synchronous roll, while for a parametric roll comparable results were obtained. However, the numerical simulation outcomes suggest that the most effective technique was the one based on FFT. The results of the applications pointed out that a proper discernment of the resonance mechanism between synchronous and parametric rolls is a key factor for choosing and executing an effective countermeasure. It is worth underlining that this paper did not account for the effects of active roll stabilisation devices; clearly, in case they were available on-board, their adoption could help in mitigating roll motion amplitude. During the simulations, a sufficient change of ship course that corresponded to an adequate modification of the heading angle, appeared more appropriate than the speed reduction in evading resonance phenomena. Particularly, for extinguishing large roll motions induced by a parametric resonance, the speed reduction approach was completely ineffective. Indeed, a course change of  $30^\circ$  was necessary to evade large roll amplitude, while for the synchronous roll case a change of course by  $15^\circ$  was sufficient.

The numerical model provided fairly accurate results, however, a further step of development should involve towing tank simulations on a scaled ship hull, to test the applicability of the proposed

detection method and to check experimentally the more reliable approach for the estimation of the wave period.

The proposed method was developed keeping in mind future industrial applications on unmanned cargo ships prone to parametric and/or synchronous roll, to help a remote crew work against excessive roll motions and accelerations. Nevertheless, the method currently could be applied to manned ships as a smart tool for supporting crew decisions in distress situations involving roll resonance phenomena.

**Author Contributions:** Conceptualization, M.A. and F.B.; methodology, M.A.; software, M.A.; validation, M.A. and F.B.; formal analysis, M.A. investigation, M.A. and F.B.; data curation, M.A.; writing—original draft preparation, M.A.; writing—review and editing, M.A. and F.B.; visualization, M.A. and F.B. All authors have read and agreed to the published version of the manuscript.

**Funding:** This research received no external funding.

**Conflicts of Interest:** The authors declare no conflict of interest.

## References

1. AAWA. *Remote and Autonomous Ships: The Next Steps*; AAWA: London, UK, 2016.
2. Felski, A.; Zwolak, K. The ocean-going autonomous ship—Challenges and threats. *J. Mar. Sci. Eng.* **2020**, *8*, 41. [\[CrossRef\]](#)
3. Glenn Wright, R. Intelligent autonomous ship navigation using multisensor modalities. *TransNav. Int. J. Mar. Navig. Saf. Sea Transp.* **2019**, *13*, 503–510. [\[CrossRef\]](#)
4. Long, M.T.; Bruhn, W.C.; Burmeister, H.C.; Long, M.T.; Moraeus, J.A. Conducting look-out on an unmanned vessel: Introduction to the advanced sensor module for Munin’s autonomous dry bulk carrier. In Proceedings of the 10th International Symposium ISIS 2014 “Integrated Ship’s Information Systems”, Hamburg, Germany, 4–5 September 2014.
5. Wróbel, K.; Montewka, J.; Kujala, P. Towards the assessment of potential impact of unmanned vessels on maritime transportation safety. *Reliab. Eng. Syst. Saf.* **2017**, *165*, 155–169. [\[CrossRef\]](#)
6. Komianos, A. The autonomous shipping era. operational, regulatory, and quality challenges. *TransNav. Int. J. Mar. Navig. Saf. Sea Transp.* **2018**. [\[CrossRef\]](#)
7. Wróbel, K.; Montewka, J.; Kujala, P. Towards the development of a system-theoretic model for safety assessment of autonomous merchant vessels. *Reliab. Eng. Syst. Saf.* **2018**, *178*, 209–224. [\[CrossRef\]](#)
8. DNV-GL. *Remote-Controlled and Autonomous Ships*; DNV-GL: Oslo, Norway, 2018.
9. Acanfora, M.; Montewka, J.; Hinz, T.; Matusiak, J. On the estimation of the design loads on container stacks due to excessive acceleration in adverse weather conditions. *Mar. Struct.* **2017**, *53*. [\[CrossRef\]](#)
10. France, W.; Levadou, M.; Treake, T.W.; Paulling, J.R.; Michel, R.K.; Moore, C. An investigation of head-sea parametric rolling and its influence on container lashing systems. *Mar. Technol.* **2003**, *40*, 1–19.
11. Acanfora, M.; Rizzuto, E. Time domain predictions of inertial loads on a drifting ship in irregular beam waves. *Ocean Eng.* **2019**, *174*, 135–147. [\[CrossRef\]](#)
12. Krata, P.; Szlapczynska, J. Ship weather routing optimization with dynamic constraints based on reliable synchronous roll prediction. *Ocean Eng.* **2018**, *150*, 124–137. [\[CrossRef\]](#)
13. Krueger, S. Evaluation of the cargo loss of a large container vessel due to parametric roll. In Proceedings of the 9th International Marine Design Conference, Dubrovnik, Croatia, 15–18 May 2006.
14. Levadou, M.; Gaillard, G. Operational guidance to avoid parametric roll. In Proceedings of the Design and Operation of Containerships, London, UK, 1 January 2003; pp. 75–86.
15. Hashimoto, H.; Umeda, N.; Ogawa, Y.; Taguchi, H.; Iseki, T.; Bulian, G.; Ishida, S.; Toki, N.; Matsuda, A. Prediction methods for parametric rolling with forward velocity and their validation—Final report of scape committee. In Proceedings of the 6th Osaka Colloquium on Seakeeping and Stability of Ships, Osaka, Japan, 26–29 March 2008.
16. Shigunov, V.; Moctar, O.E.; Rathje, H. Operational guidance for prevention of cargo loss and damage on container ships. *Sh. Technol. Res.* **2010**, *57*, 8–25. [\[CrossRef\]](#)
17. Acanfora, M.; Montewka, J.; Hinz, T.; Matusiak, J. Towards realistic estimation of ship excessive motions in heavy weather. A case study of a containership in the Pacific Ocean. *Ocean Eng.* **2017**, *138*. [\[CrossRef\]](#)

18. Belenky, V.; Yu, H.-C.; Weems, K. Numerical procedures and practical experience of assessment of parametric roll of container carriers. In Proceedings of the 9th International Conference on Stability of Ships and Ocean Vehicles, Rio de Janeiro, Brazil, 25–29 September 2006.
19. Galeazzi, R.; Blanke, M.; Poulsen, N.K. Early detection of parametric roll resonance on container ships. *IEEE Trans. Control Syst. Technol.* **2013**, *21*, 489–503. [\[CrossRef\]](#)
20. Galeazzi, R.; Blanke, M.; Poulsen, N.K. Detection of parametric roll for ships. In *Parametric Resonance in Dynamical System*; Fossen, T.I., Nijmeijer, H., Eds.; Springer: Berlin/Heidelberg, Germany, 2012; ISBN 978-1-4614-1042-3.
21. McCue, L.S.; Bulian, G. A numerical feasibility study of a parametric roll advance warning system. *J. Offshore Mech. Arct. Eng.* **2007**, *129*, 165. [\[CrossRef\]](#)
22. Hashimoto, H.; Taniguchi, Y.; Fujii, M. A case study on operational limitations by means of navigation simulation. In Proceedings of the 16th International Ship Stability Workshop (ISSW2017), Belgrade, Serbia, 5–7 June 2017; pp. 5–7.
23. Nielsen, U.D.; Brodtkorb, A.H.; Sørensen, A.J. Sea state estimation using multiple ships simultaneously as sailing wave buoys. *Appl. Ocean Res.* **2019**, *83*, 65–76. [\[CrossRef\]](#)
24. Nielsen, U.D. Estimations of on-site directional wave spectra from measured ship responses. *Mar. Struct.* **2006**, *19*, 33–69. [\[CrossRef\]](#)
25. Acanfora, M.; Krata, P.; Montewka, J.; Kujala, P. Towards a method for detecting large roll motions suitable for oceangoing ships. *Appl. Ocean Res.* **2018**, *79*, 49–61. [\[CrossRef\]](#)
26. Fossen, T.I. *Guidance and Control of Ocean Vehicles*; Wiley: Chichester, UK, 1996; ISBN 0-471-94113-1.
27. Matusiak, J.; Stigler, C. Ship roll motion in irregular waves during a turning circle maneuver. In Proceedings of the 11th International Conference on Stability of Ships and Ocean Vehicles, Athens, Greece, 23–28 September 2012; pp. 291–298.
28. Stigler, C. *Investigation of the Behaviour of a RoPax Vessel in Stern Quartering Irregular Long-Crested Waves*; Aalto University: Espoo, Finland, 2012.
29. Matusiak, J. *Dynamics of a Rigid Ship*; Aalto University Publication Series: Science + Technology: Espoo, Finland, 2013; ISBN 9789526052045.
30. Acanfora, M.; Matusiak, J. On the estimations of ship motions during maneuvering tasks in irregular seas. In Proceedings of the 3rd International Conference on Maritime Technology and Engineering, Lisbon, Portugal, 4–6 July 2016; Volume 1.
31. ITTC The Specialist Committee on Prediction of Extreme Ship Motions and Capsizing Final Report and Recommendations to the 23rd ITTC. In Proceedings of the 23rd International Towing Tank Conference, Venice, Italy, 8–14 September 2002; Volume II, pp. 619–748.
32. Spanos, D.; Palmquist, M. Benchmark Study on Numerical Simulation Methods for the Prediction of Parametric Roll of Ships in Waves. In Proceedings of the 10th International Conference on Stability of Ships and Ocean Vehicles, Sankt Petersburg, Russia, 22–26 June 2009; pp. 1–9.
33. Shigunov, V.; el Moctar, O.; Papanikolaou, A.; Potthoff, R.; Liu, S. International benchmark study on numerical simulation methods for prediction of manoeuvrability of ships in waves. *Ocean Eng.* **2018**, *165*, 365–385. [\[CrossRef\]](#)
34. Cummins, W.E. *The Impulse Response Function and Ship Motions*; Institut für Schiffbau der Universität Hamburg: Hamburg, Germany, 1962; Volume 57.
35. RINA. *RINA Rules, Steering Gear, Part C, Chapter 1, Section 11*; RINA: Genoa, Italy, 2017.
36. Chen, G.; Wang, Z. A signal decomposition theorem with Hilbert transform and its application to narrowband time series with closely spaced frequency components. *Mech. Syst. Signal Process.* **2012**, *28*, 258–279. [\[CrossRef\]](#)

